Overview of Evaluation of Pile Foundation Stiffnesses for Seismic Analysis of Highway Bridges

GARY M. NORRIS

Methods for the assessment of the nonlinear variation in pile foundation stiffnesses are presented. Values of such lateral and vertical/rotational stiffnesses are intended for use for boundary element springs of a structural dynamic model of a highway bridge undergoing seismic analysis. Conflicts between the FHWA and Applied Technology Council approaches to foundation stiffness evaluation as well as deficiencies in these methods are noted. The methodology presented is demonstrated relative to a number of field case studies that have backcalculated values (or other responses) with which to compare. Such field case studies involve both failing and nonfailing soil responses, different soil conditions, a wide range of deflection amplitudes, and different types of loading (ambient level tests, full-scale, push-back, quick-release bridge tests, and response during earthquake excitation).

Foundation flexibility is taken into account in the structural dynamic modeling of a pile-supported highway bridge by incorporating boundary element springs of stiffness values comparable with those of the soil-pile foundation systems they replace. Typically, the lateral and rotational stiffnesses of the foundations are required for the seismic analysis of a highway bridge.

Whereas the bridge designer undertakes the dynamic analysis of the structure, the geotechnical engineer should direct the evaluation of the foundation stiffnesses needed in the analysis. Given the nonlinear variation of the soil modulus, the dependence of such modulus values on the stress path and the near-field soil strain (associated with superposed free-field and inertial interaction responses), and the necessity of evaluating such modulus dependence from relatively meager subsurface data, such geotechnical expertise is critical. Since the geotechnical engineer evaluates the site-dependent free-field ground surface motions or response spectrum to be used as input to the structure, he already has knowledge of the level of free-field strains that will develop in the different soil layers.

What is needed for realistic structural dynamic modeling is an accurate assessment of both the ground surface motions and the foundation stiffnesses along the length of the structure so that the dynamic analysis leads to an appropriate distribution of seismic forces to the structure. Unfortunately, the bridge design group often chooses to do a fixed base (i.e., infinitely stiff springs) response evaluation or, alternatively, undertakes the evaluation of the foundation springs for what it considers a worst-case soil condition. Neither approach is to be encouraged because each can lead to significant inaccuracies. In fact, it is not presently known whether an evaluation of the foundation springs for spatially varying soil conditions using linear "design level" stiffnesses with limiting force or moment capacity is sufficient for the task. It may be that a full equivalent linear stiffness analysis, similar in principle to the use of strain compatible shear moduli in a ground response analysis, is required.

Geotechnical input into pile foundation stiffness evaluation is necessary if the potential for a commonly overlooked mechanism of failure is to be assessed. There can be situations where, because of softening of the soil profile associated with either cyclically degrading clay or developing but unrealized liquefaction in sand, the combination of the inertial interaction load from the superstructure and the reduced strength of the soil results in a foundation failure as seen, for instance, in Mexico City in 1985. Accordingly, there might not be free-field soil failure (e.g., liquefaction) or failure initiating with the superstructure, but rather a soil-foundation interaction failure that might be overlooked given the traditional division of work between the bridge design and geotechnical groups within a highway department. Such consideration of soil-foundation interaction failure can be treated in the context of a geotechnical pile foundation stiffness evaluation as shown in the published Meloland, Oakland Outer Harbor, and Cypress case studies.

This paper provides an overview of the author's equivalent linear lateral and rotational pile foundation stiffness evaluation procedures (*1*) and some field case studies (*1–4*).

UNCOUPLED STIFFNESSES AND DIFFERENCES IN ASSOCIATED EFFECTS

It is assumed that the lateral and rotational responses of a pile group can be uncoupled and treated independently (Figure 1a) provided that there are no batter piles in the group. Accordingly, the lateral response of the group derives from the soil-pile interaction of the piles near ground surface (together with the lateral resistance of the pile cap and any embedded portion of the pier shaft). The rotational resistance of the group, on the other hand, is dominated by the axial (i.e., vertical) response of the piles about the corresponding axis of rotation. The soils at depth provide the significant part of the axial and, hence, the rotational stiffness of the group.

The associated near-field zones of soil that govern in lateral versus vertical/rotational stiffness evaluation are shown in Figure 1b. The soil modulus variation in these different zones

University of Nevada, Reno, Nev. 89557.

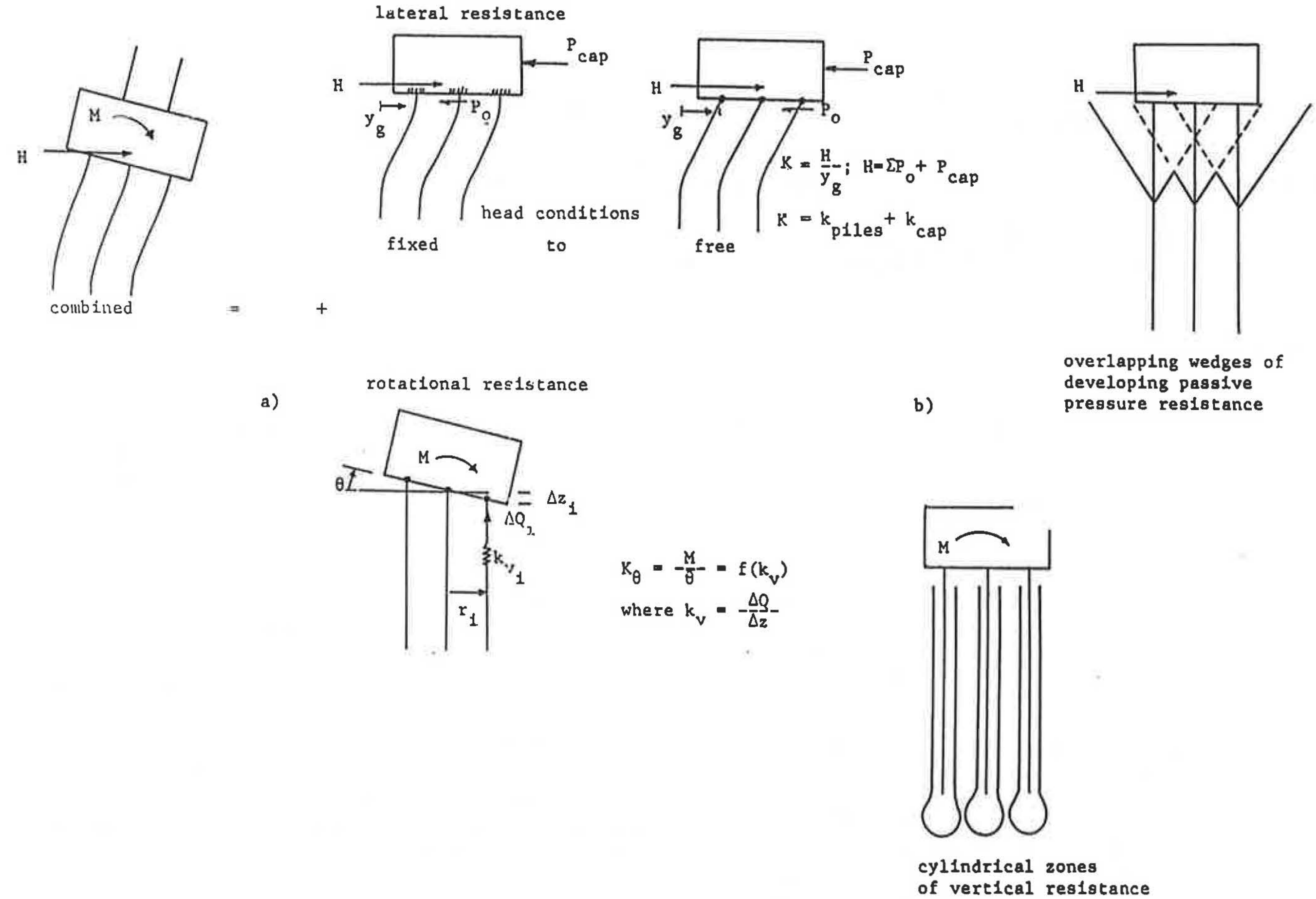

FIGURE 1 (a) Uncoupled lateral and rotational responses and (b) associated zones of soil-pile interaction.

governs the respective pile foundation stiffness evaluations. Furthermore, pile group interference effects, head fixity conditions, and the pile cap contribution are different for the different modes. Group interference due to the progressive overlap of developing passive wedges can be significant for lateral response, whereas there is negligible interaction of cylindrical zones and point pressure bulbs with respect to vertical and, hence, rotational pile group response (Figure 1b). Pile head fixity, ranging from a pinned to a fully fixed condition, has little effect with respect to the rotational stiffness of the pile group; therefore, a pinned condition is assumed. On the other hand, lateral stiffness will vary significantly depending on the assumed head fixity condition (Figure 1a). In fact, the head fixity of a given pile group may vary from being fixed to tending toward a free or pinned head response with an increasing lateral load.

It is assumed here that the soil settles away from the base of the pile cap and that, because of a concurrent lateral response (i.e., the development of soil gaps along the vertical faces of the cap), there is no pile cap contribution to rotational stiffness. On the other hand, with the soil gap closed, there will be a developing passive wedge in front of the leading face of the pile cap resulting in a notable pile cap contribution to lateral resistance. However, such lateral pile cap resistance should not include the shear along its base because, even if the soil does not settle away from the cap, the soil moves laterally with the cap because of the soil deformation associated with the lateral movement of the underlying piles. Accordingly, it is inappropriate to evaluate the lateral stiffness of the pile cap by treating it as an embedded shallow foundation with base shear as proposed by FHWA (*5*). Furthermore, the choice of the soil modulus value for cap resistance should be made in conjunction with the level of the lateral deflection of the cap, which is equal to that of the piles at pile top. Given the difference in the width of the pile cap versus the individual pile, the same displacement implies that decidedly different soil strains (proportional to the deflection divided by the width of the member) and, hence, modulus values occur in the controlling zones of the soil in front of the cap versus the individual pile.

BEAM-ON-ELASTIC FOUNDATION FORMULATION

Lateral and rotation pile group stiffnesses rely on first assessing the nonlinear variation in lateral and vertical pile responses. This is best achieved by using the well-accepted beam-on-elastic foundation (BEF) formulation, in which soil-pile reactions are characterized by a continuous bed of springs.

Given the uncoupling of the lateral and rotational responses of the pile group, different sets of springs are used to characterize the lateral (i.e., *p-y*) and the vertical (*t-z*) soil-pile reactions (Figure 2).

One significant difference between the lateral and vertical pile responses is that the piles are under an initial static vertical load. Therefore, of the two different pile head responses,

- The horizontal load-displacement (P_o-y_o) response (or the associated pile head stiffness, $k = P_o/y_o$) from *p-y* behavior and
- The vertical load change-displacement (ΔQ-Δz) response (or the associated vertical pile head stiffness, $k_v = \Delta Q/\Delta z$) from *t-z* behavior,

the vertical will be different in unload versus load behavior in accordance with the subsequent inertial interaction loading of the pile group (Figure 2b). The consequences of this are considered in a later section.

LATERAL STIFFNESS EVALUATION

Currently available *p-y* curve formulation (*5*) has several limitations relative to its use in highway bridge seismic pile foundation analysis. Such formulation was not meant to be particularly accurate in the small deflection range, nor are such *p-y* curves appropriate for an embedded pile head (i.e., with the pile top occurring at the base of the cap at, say, 5 to 10 ft below the ground surface). Likewise, available *p-y* curve formulation does not account for differences in the pile bending stiffness (EI), the pile shape, and the pile head fixity. Whereas strain wedge (SW) model formulation (*3,4*) will account for all of these factors, such refinement may not be warranted given the subsequent modification due to pile group interference effects and due to existing differences in opinion as to the contribution of the pile cap (*1,5*).

A simple but realistic *p-y* BEF analysis that addresses both the small deflection and embedment issues is the equivalent linear subgrade modulus profile approach (*1*). Accordingly, one assesses the design level subgrade modulus, $E_s(= p/y)$ profiles [i.e., $E_s = fx$ (Figure 3a)] given the modulus variation f as characterized in the literature (Figure 4a). However, only that portion of the profile from the pile top and down is used to assess the isolated pile stiffness, k, whereas that variation over the height of the pile cap is used to evaluate the contribution of the pile cap, k_{cap}. Such a design level modulus profile applies at a given value of strain in the soil in the developing passive wedge in front of the pile (or pile cap), which reflects a pile head (or cap) deflection, y_o (or y_g), of 0.1 in./ft of pile (or cap) width B. At a lesser value of deflection, the soil strain is less and the modulus profile is stiffer

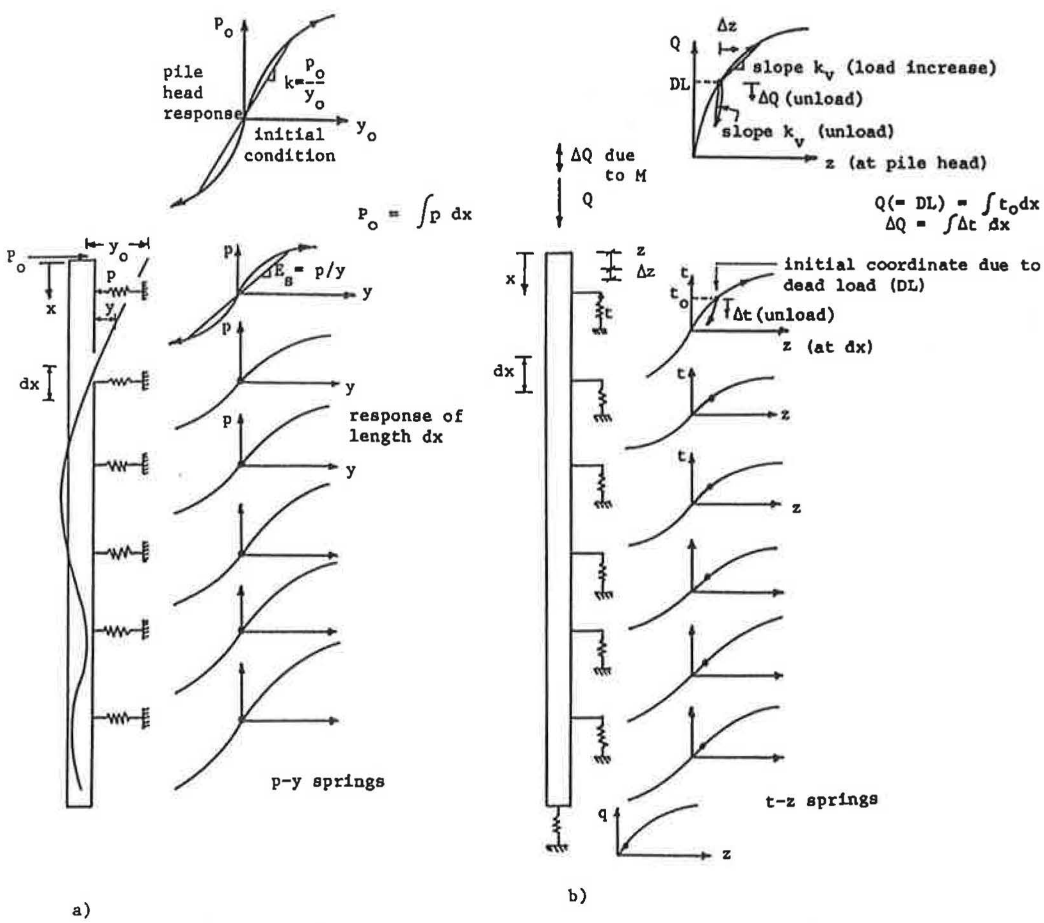

FIGURE 2 BEF characterization for (a) lateral and (b) vertical single pile response.

(Figure 3b) where such a modulus profile amplification value is assessed from Figure 4b given the deflection y_o (y_g) and pile (or cap) width B of interest.

The stiffness, K, of the pile group at a deflection y_g of the pile cap (the same as the deflection at the top of the piles) is

$$K = k_{\text{piles}} + k_{\text{cap}} \tag{1}$$

where K_{piles} is the stiffness of the n number of piles in the group considered collectively, and k_{cap} is the stiffness generated because of the lateral resistance along the vertical side of the front of the pile cap and any embedded portion of the pier shaft. The stiffness of the piles, k_{piles}, is n times the stiffness of the average group pile, k_{gp}, or n times the stiffness of the isolated pile, k, times a group reduction factor, e_g, that takes into account group interference effects, that is

$$k_{\text{piles}} = nk_{gp} = e_g nk \tag{2}$$

The factor e_g applies at the same load per pile to the group pile as to the isolated pile and, therefore, at a displacement y_g of the pile in the group as compared with the pile top displacement, y_o, of the isolated pile, that is,

$$k_{gp} = e_g k$$

where k_{gp} applies at displacement y_g (i.e., $k_{gp} = P_o/y_g$), k applies at displacement y_o (i.e., $k = P_o/y_o$), and

$$y_o = e_g y_g \tag{3}$$

The relationship between (k,y_o) of the isolated pile and (k_{gp},y_g) of the pile in the group is shown in Figure 5. Factor e_g is a function of pile spacing and is equal to 0.354, 0.503, 0.639, 0.765, 0.885, and 1 for pile spacing, S, of 3, 4, 5, 6, 7, and 8 pile diameters, B, respectively.

From BEF theory, the stiffness of the single isolated pile, k, at a pile top displacement, y_o, can be expressed as

$$k = \frac{EI}{(A_{yo} \text{ or } C_{yo})T^3} \tag{4}$$

where EI is the bending stiffness of the pile in units of F/L², A_{yo} (or C_{yo}) is the dimensionless BEF coefficient of displacement for free (or fixed) head conditions, and T is the relative stiffness factor of the pile in units of L. The equation for T and the value of coefficients A_{yo} and C_{yo} are established from a collection of published solutions (*1*) for different shaped E_s profiles.

The pile cap stiffness, k_{cap}, due to a uniform horizontal translation, y_g, of the pile cap is

$$k_{\text{cap}} = \frac{P_{\text{cap}}}{y_g} \tag{5}$$

where

$$P_{\text{cap}} = \int p \, dx \tag{6}$$

is the force associated with the integration of the line load force, p (in units of F/L), over the height of the cap and any embedded portion of the pier shaft. Note that p of the p-y curve is

$$p = E_s y \tag{7}$$

(Figure 2a) as in the fashion of the laterally loaded pile but that $y = y_g$ and $E_s = fx$ (see Figure 3a) where f (Figure 4a) now corresponds to the deflection $y_{g,\text{design}}$ = 0.1 in. × B(ft)/1 ft, where B is taken as the width of the pile cap. Using the appropriate modulus amplification curve of Figure 4b, one

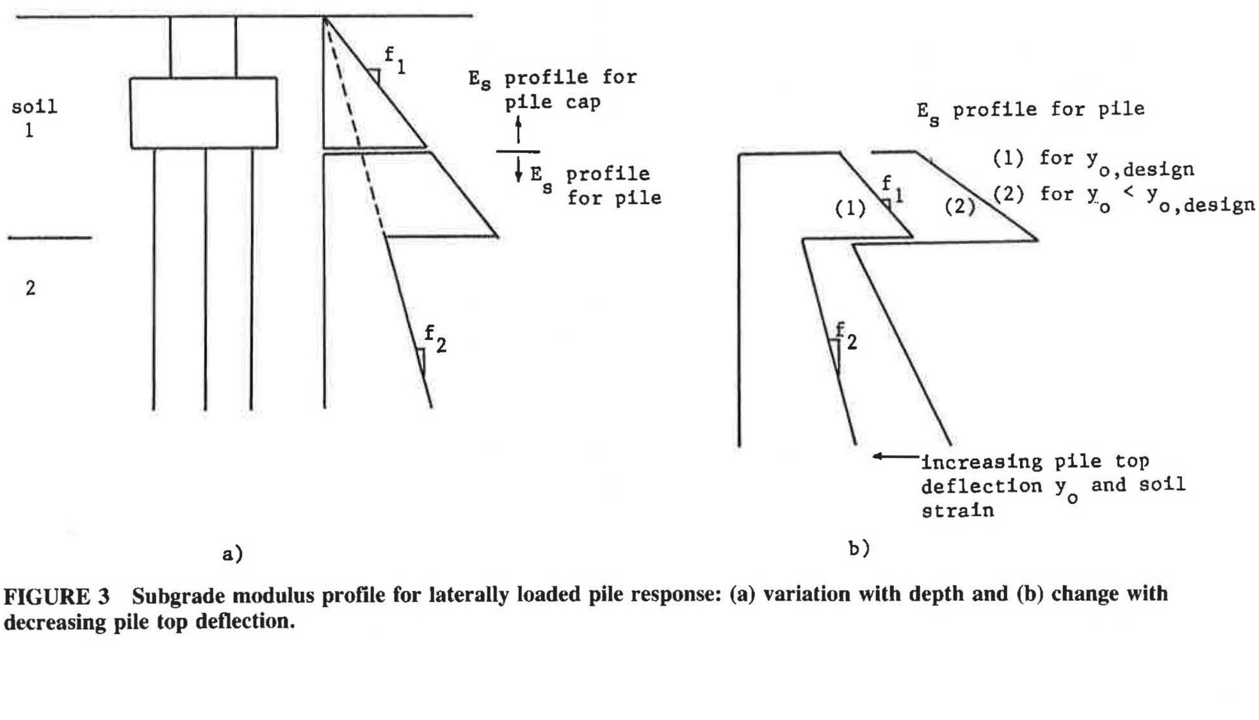

FIGURE 3 Subgrade modulus profile for laterally loaded pile response: (a) variation with depth and (b) change with decreasing pile top deflection.

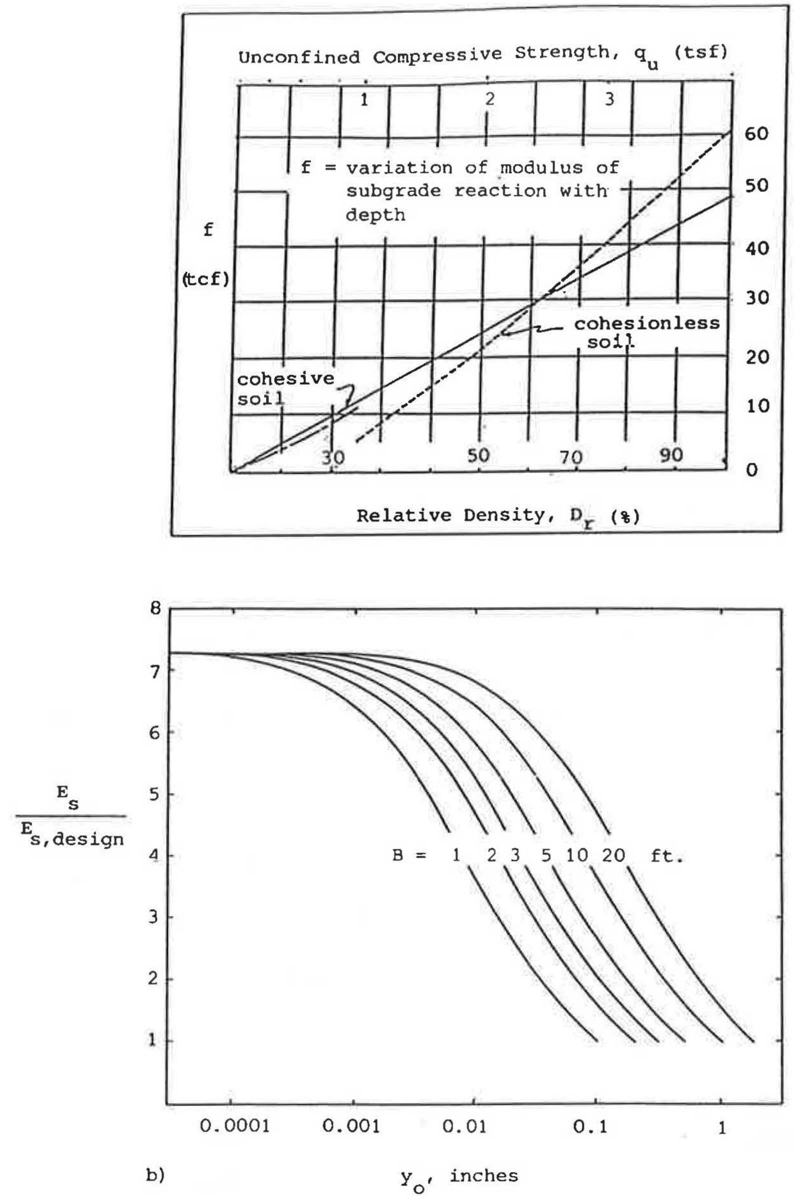

FIGURE 4 (a) Design level subgrade modulus Variation f and (b) subgrade modulus amplification curves (*1*).

can then obtain the E_s profile for the cap corresponding to the desired value of deflection, y_g, of the pile group. Thereafter, k_{cap} (upon substitution of Equation 7 into Equation 6 and Equation 6 into Equation 5) becomes

$$k_{cap} = (1/y_g)\int E_s y_g dx = \int E_s dx \qquad (8)$$

A step-by-step outline of the foregoing procedure as well as sample calculations for the determination of the lateral stiffnesses for Pile Groups 1 and 2 of the Rose Creek Bridge is provided elsewhere (*1*). Figure 6 compares the predicted range in stiffness variations (from free to fixed head conditions based upon the aforementioned procedure) with best fit values for Piles Groups 1 through 4 backcalculated from system ID evaluation of bridge response data from full-scale, high-amplitude, push-back, quick-release field tests of the bridge (*6*). Such bridge tests were carried out over a range in release displacements.

The predicted curves of Figure 6 were obtained using only simple hand calculations and commonly available soil data as provided in the boring logs from the bridge plans. Such equivalent linear stiffness evaluation takes only slightly longer than evaluating just the design level stiffnesses (values at the right end of the curves). In the context of the recommended use of such lateral stiffness (and comparable rotational stiffness) curves, a linear structural dynamic analysis would be undertaken using an assumed set of pile foundation stiffnesses and free-field motion input. Such linear dynamic analysis would be repeated until convergence in the assumed and displace-

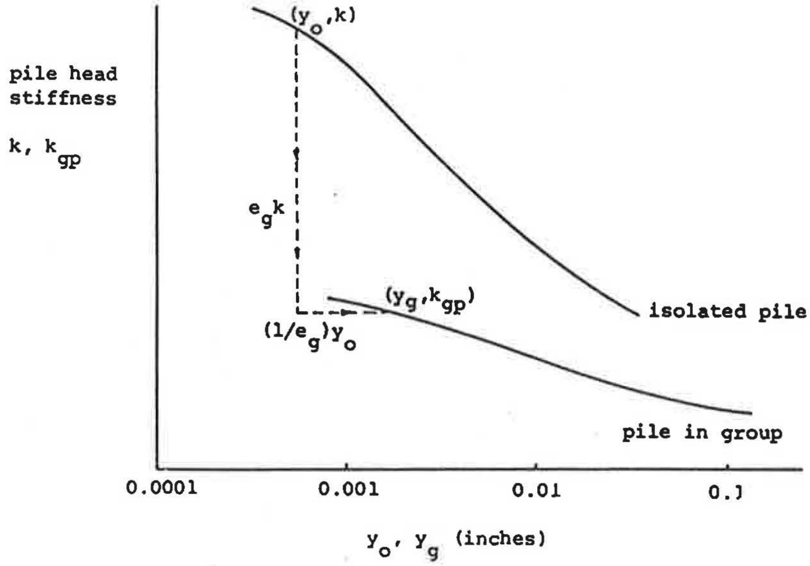

FIGURE 5 Pile head stiffness versus pile top deflection for the single isolated pile (k versus y_o) and the pile in the group (k_{gp} versus y_g).

ment compatible stiffnesses results. (The effect of using displacement compatible versus design level stiffnesses might then be judged.)

The equivalent linear subgrade modulus profile approach is the equivalent of generating the *p-y* curves with depth but with embedment effects handled directly. In addition, because the modulus amplification curve (Figure 4b) is modeled after the shear modulus reduction curve from soil dynamics, small strain/deflection response is appropriately characterized.

ROTATIONAL STIFFNESS EVALUATION

The rotational stiffness, K_θ, of a pile group is the ratio of the applied moment, M, to the resulting rotation, θ, of the base of the pile cap:

$$K_\theta = M/\theta \tag{9}$$

As discussed earlier, assuming the piles to be pin ended in a rigid pile cap and no cap contribution, the resistance to moment, M, derives solely from the axial response of the (vertical) piles. Given that the pile group is under initial static dead load corresponding to an average pile head force, Q, the moment resistance (equal to M) is the product of the load change, ΔQ_i, in each pile and the distance, r_i, of the pile from the axis of rotation summed over all the piles in the group:

$$M = \sum \Delta Q_i r_i \tag{10}$$

Given that the vertical axial stiffness at the pile head is $k_{vi} = \Delta Q_i/\Delta z_i$, where Δz_i is the pile head displacement, then $\Delta Q_i = k_{vi}\Delta z_i$, so that Equation 10 can be expressed as

$$M = \sum k_{vi}\Delta z_i r_i \tag{11}$$

The relationship between the pile head displacement, Δz_i, and the rotation, θ, is

$$\Delta z_i = r_i\theta \tag{12}$$

Substituting Equation 12 into Equation 11 yields

$$M = \sum k_{vi} r_i^2 \theta \tag{13}$$

and substituting Equation 13 into Equation 9 yields

$$K_\theta = \sum k_{vi} r_i^2 \tag{14}$$

Due to the initial dead load, Q, on the piles, there are different vertical stiffnesses, k_v, in load versus unload response associated with moment, M (Figure 2b). Consequently, the axis of rotation of a regular arrangement of piles is not the symmetrical center of the group. (The axis is shifted toward the stiffer unload piles.) Furthermore, once the moment is reversed, the piles that have unloaded reload and the piles that have undergone a load increase unload so that the axis shifts from its original position to a new one. Figure 7, for instance, shows the *Q-z* travel paths of the piles of a two-row pile group and the associated M-θ response of the group under cyclic θ excitation (Figure 7a). (Points numbered 1 through 14 in Figures 7a and 7e correspond to those in Figure 7d.) However, in two to three cycles, the M-θ response stiffens in association with the piles tending toward the same (stabilized) unload-reload *Q-z* travel path (*x-y* in Figure 7d) corresponding to a centrally located axis of rotation. The stabilized stiffness, $K_\theta = M/\theta$ (Figure 7e), is of interest here. Given that the stabilized rotational stiffness of the pile group is a function of the stabilized unload-reload axial pile stiffness, $k_{u/r}$ (slope *x-y* in Figure 7d), Equation 14 (for stabilized response) becomes

$$K_\theta = \sum k_{u/r,i} r_i^2 \tag{15}$$

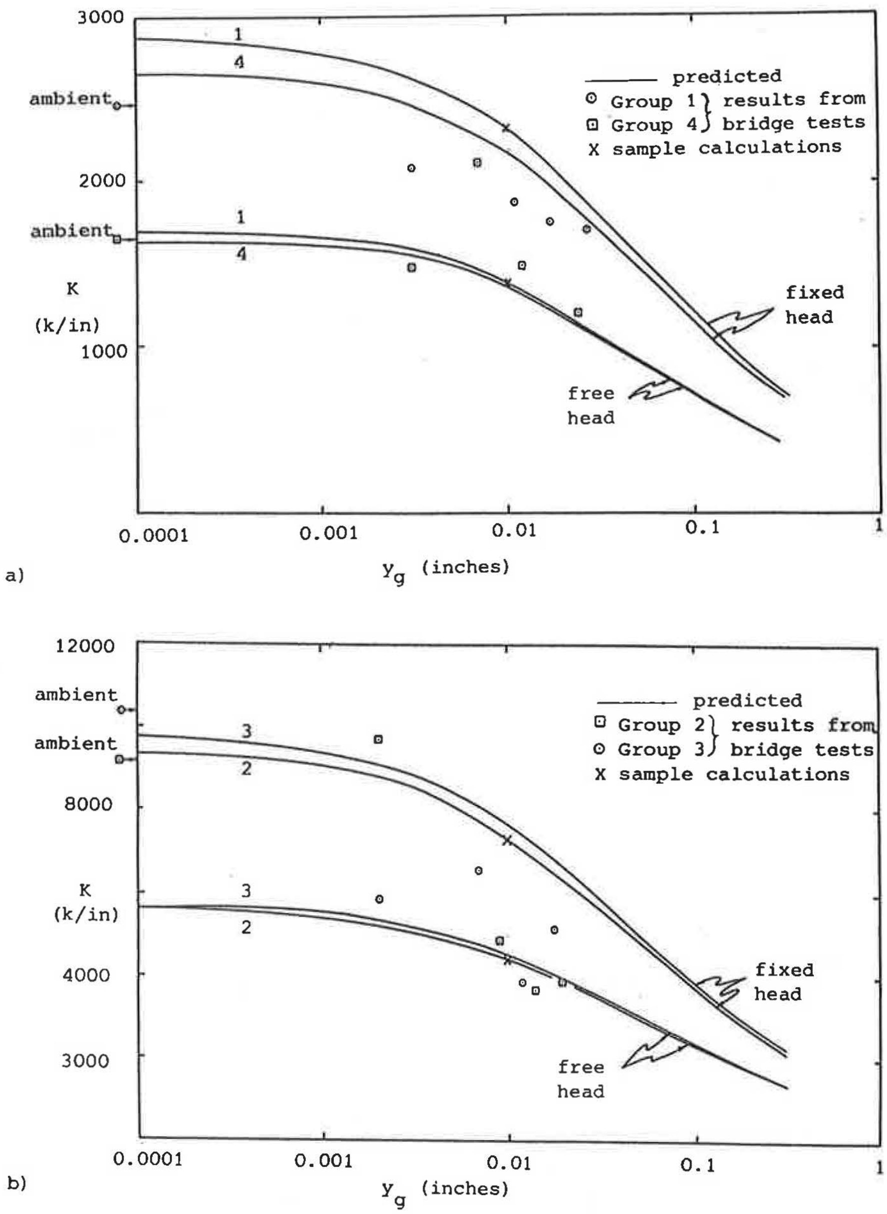

FIGURE 6 Comparison of predicted versus observed (i.e., backcalculated) lateral stiffness results from (a) Pile Groups 1 and 4 and (b) Pile Groups 2 and 3 of the Rose Creek Bridge (*1*).

Whereas the Q-z travel paths and the M-θ changes of Figures 7d and 7e are shown as straight line segments, they are only the secant slopes of the actual nonlinear variation. Therefore, the value of $_{k_{u/r}}$ actually varies (from one pile row to the next) with the amplitude of unload-reload displacement, $\Delta z_{u/r}$ ($= r_i\theta$), as shown, for example, in Figure 8 for the piles of Pile Groups 1 through 4 of the Rose Creek Bridge.

Norris (1) presents a method for the assessment of the nonlinear variation in the unload-reload axial pile stiffness, $k_{u/r}$. The method is based on using Ramberg-Osgood formulation relative to the backbone Coyle-Reese (clay) t-z curves, from which one can then establish the unload-reload t-z response (Figure 2b). This includes the use of small amplitude shear stress-shear strain theory to accurately extend formulation of the Coyle-Reese t-z curves to include nonlinear small amplitude t-z response. Given that using the backbone t-z responses in a Coyle-Reese type of analysis yields the backbone pile head Q-z response (Figure 2b), then, by using the unload-reload Δt-Δz response, one obtains the corresponding $\Delta Q_{u/r}$-$\Delta z_{u/r}$ pile head response and, therefore, $k_{u/r}$ ($= \Delta Q_{u/r}/\Delta z_{u/r}$). Norris (*1*) presents a detailed outline of the associated solution procedure, a listing of a very short but useful BASIC program, and a worked example. The $k_{u/r}$ versus $\Delta z_{u/r}$ responses shown in Figure 8 for Pile Groups 1 through 4 of the Rose Creek Bridge were obtained using this procedure. On the basis of Equation 15, the rotational stiffness variations, k_θ versus θ (Figure 9), for Groups 1 through 4 were assessed. They are compared with values backcalculated from

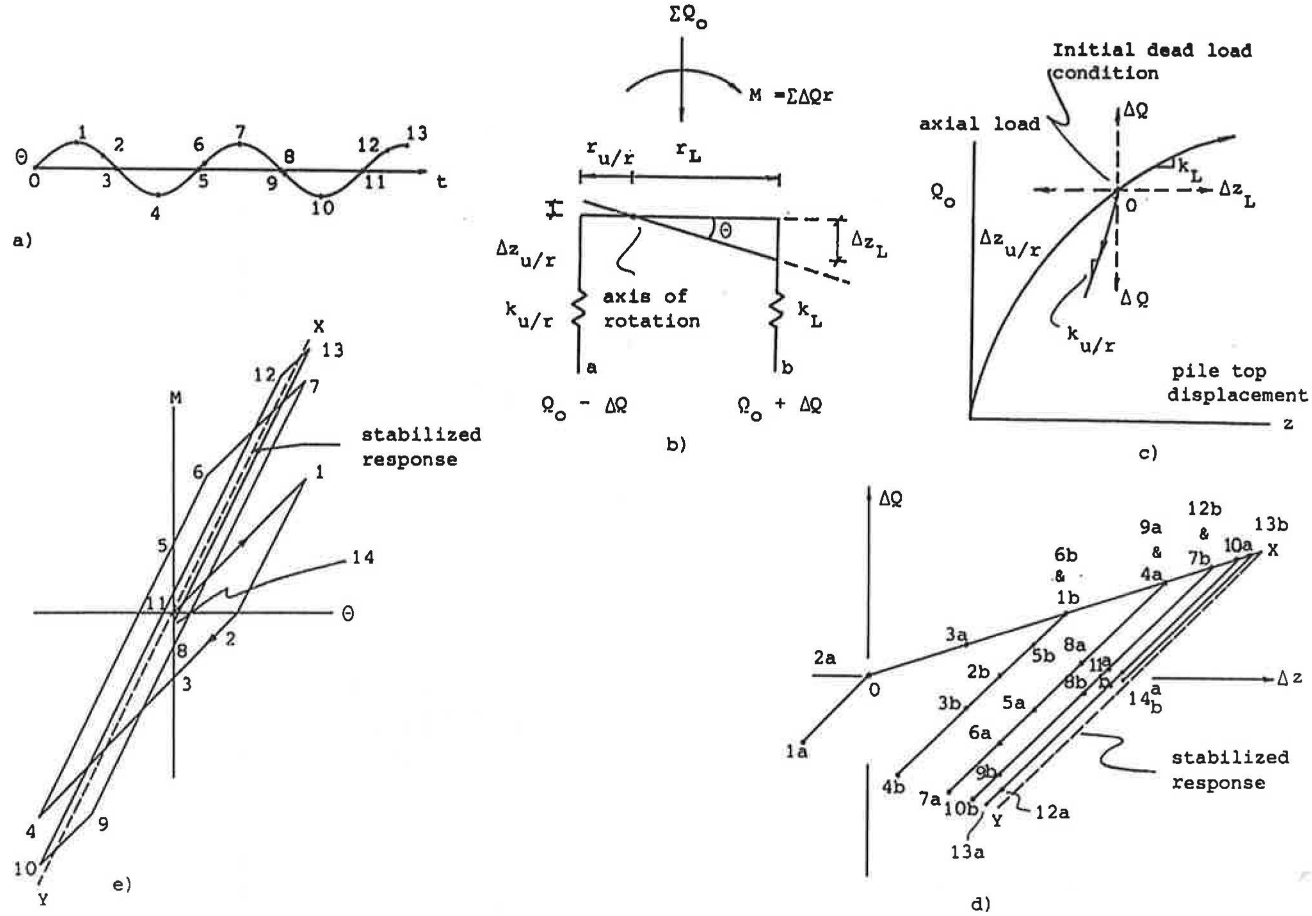

FIGURE 7 (a) Rotational excitation of (b) a two-row pile group given (c) the backbone load-displacement (Q-z) response of the piles with (d) the Q-z travel paths of Row a and b piles in the proximity of the initial condition and (e) the corresponding M-θ response.

the system ID evaluation of bridge response data from the same full-scale, high-amplitude, push-back, quick-release field tests mentioned earlier. The best fit backcalculated rotational stiffness values shown here imply simultaneous adoption of the best fit lateral stiffness values of Figure 6, and vice versa.

An interesting phenomenon is associated with Figures 7d and 7e. Over the two to three cycles necessary for stabilized behavior to develop, (*a*) permanent rotationally induced settlement develops (equal to the horizontal distance between Point 0 and a point on the *x*-*y* line directly to the right of points 14a and 14b of Figure 7d); (*b*) the spring stiffness, K_θ, increases (i.e., the secant slope between Points 1 and 4, then Points 7 and 10, and then *x*-*y* of Figure 7e increases); and (*c*) a mechanism of damping (as judged by the diminishing area of the M-θ loops of Figure 7e) develops that is not attributable to traditional material or geometric sources. It may be important in future applications to take account of such a response.

STIFFNESS AS A FUNCTION OF NEAR VERSUS FAR-FIELD SOIL RESPONSE

Given that the lateral resistance of the piles derives from the developing passive soil wedges near the ground surface and that the axial (and, hence, the rotational) resistance of the piles derives from the cylindrical zones of soil over the full length of the piles (Figure 1b), it is clear that the lateral and rotational stiffnesses of the pile group depend on the nonlinear soil properties (a function of the stress or strain level) within these regions thus affected by soil-structure interaction response. However, in an earthquake, the "far" or "free" field soil is also moving. Therefore, for seismic excitation, one should actually take the modulus within a given region to be a function of the total strain, where the total strain is equal to the algebraic sum of the free-field and the inertial interaction strains (with due regard for phase differences). Unfortunately, such an evaluation is not presently feasible, which has led to the development of two conflicting approaches.

FHWA (*5*) has recommended that pile foundation stiffnesses be assessed on the basis of BEF (*p*-*y* and *t*-*z* type) analyses. Such nonlinear analyses require soil parameter input that is a function of the relative (or inertial interaction) displacement/strain. Therefore, the resulting lateral or rotational stiffness plotted as a function of relative displacement/rotation would vary as shown by the curve designated "FHWA" in Figure 10a. The Applied Technology Council (ATC) (*7*), on the other hand, recommends that stiffnesses be assessed on the basis of soil modulus values chosen as a function of the

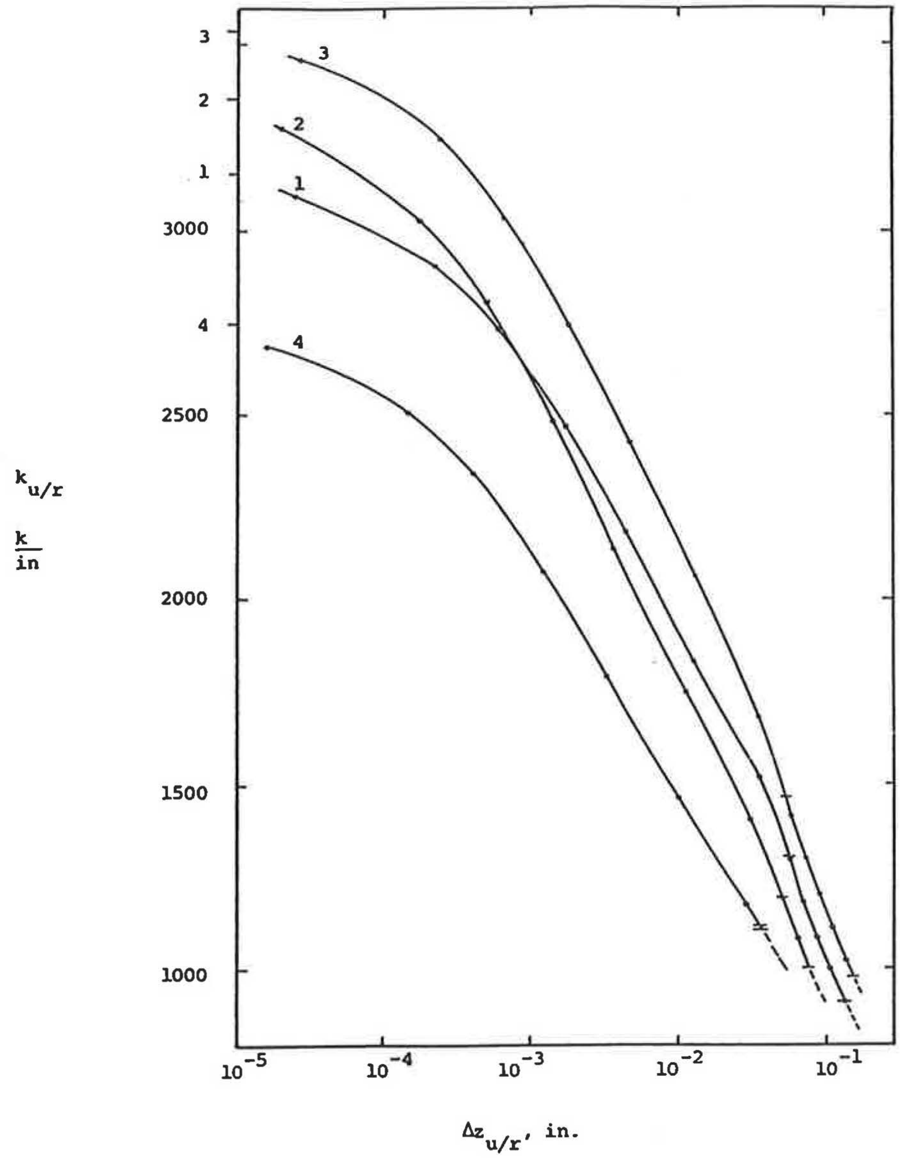

FIGURE 8 Vertical pile head stiffness $k_{u/r}$ versus $\Delta z_{u/r}$ curves for piles of Groups 1-4 from Rose Creek (*1*).

free-field level of soil strain as assessed, for instance, in a ground response analysis. Such a stiffness would be independent of the relative displacement/rotation and would plot as a horizontal line (a constant value) across Figure 10a. As an expedient, it appears that a combination of the two approaches would be more appropriate. For lower levels of relative displacement (or relative strain), the far- (or free-) field strain would be larger and, therefore, the combined strain would be closer to the free-field value. This implies that the ATC (constant) variation is applicable on the far left-hand side of Figure 10a. At larger levels of inertial interaction displacement/rotation (on the right side of Figure 10a), the relative strain dominates and the FHWA approach should be used. At the intersection of the ATC and FHWA variations, the free-field and relative strains are equal, and the combined strain will depend on the phase difference between the two components. At present, the author assumes a direct transition from the ATC to the FHWA variation, as shown in Figure 10b.

In the comparison of the predicted and backcalculated lateral and rotational stiffnesses of Figures 6, 8, and 9 from the Rose Creek Bridge field tests, only relative strains were induced in the soil, and, therefore, no horizontal (ATC-type) cap on the predicted curves was used. Depending on the level of free-field motions to be considered, a cap would need to be superposed. Such discussion points out the possibility for error if backcalculated stiffnesses from full-scale bridge tests are used in seismic without modification.

Analysis of the Oakland Outer Harbor Wharf (*3*), an instrumented structure that was shaken in the Loma Prieta earthquake, provides an example of the need for such a distinction between the free-field and near-field soil strains. Fig-

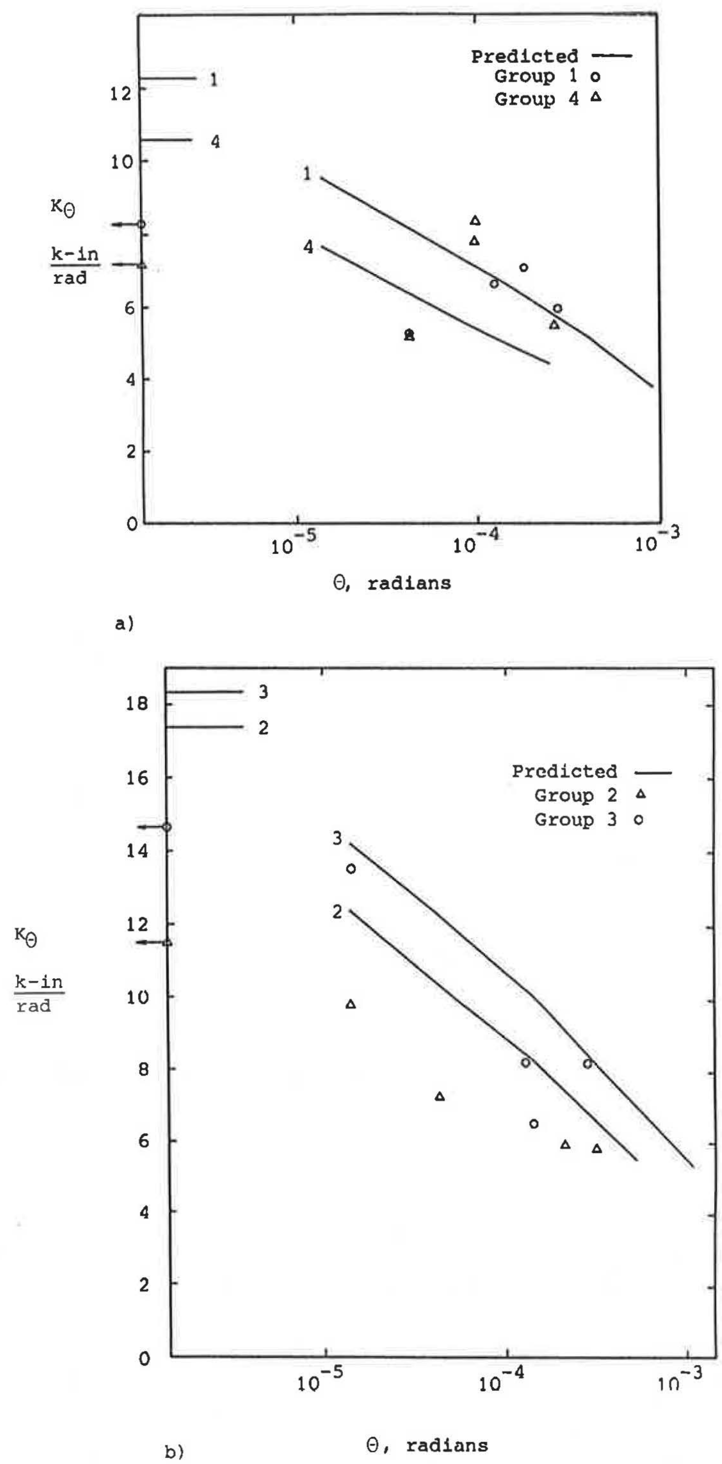

FIGURE 9 Comparison of predicted versus observed (i.e., backcalculated) rotational stiffness values for (a) Pile Groups 1 and 4 and (b) Pile Groups 2 and 3 of the Rose Creek Bridge (*1*).

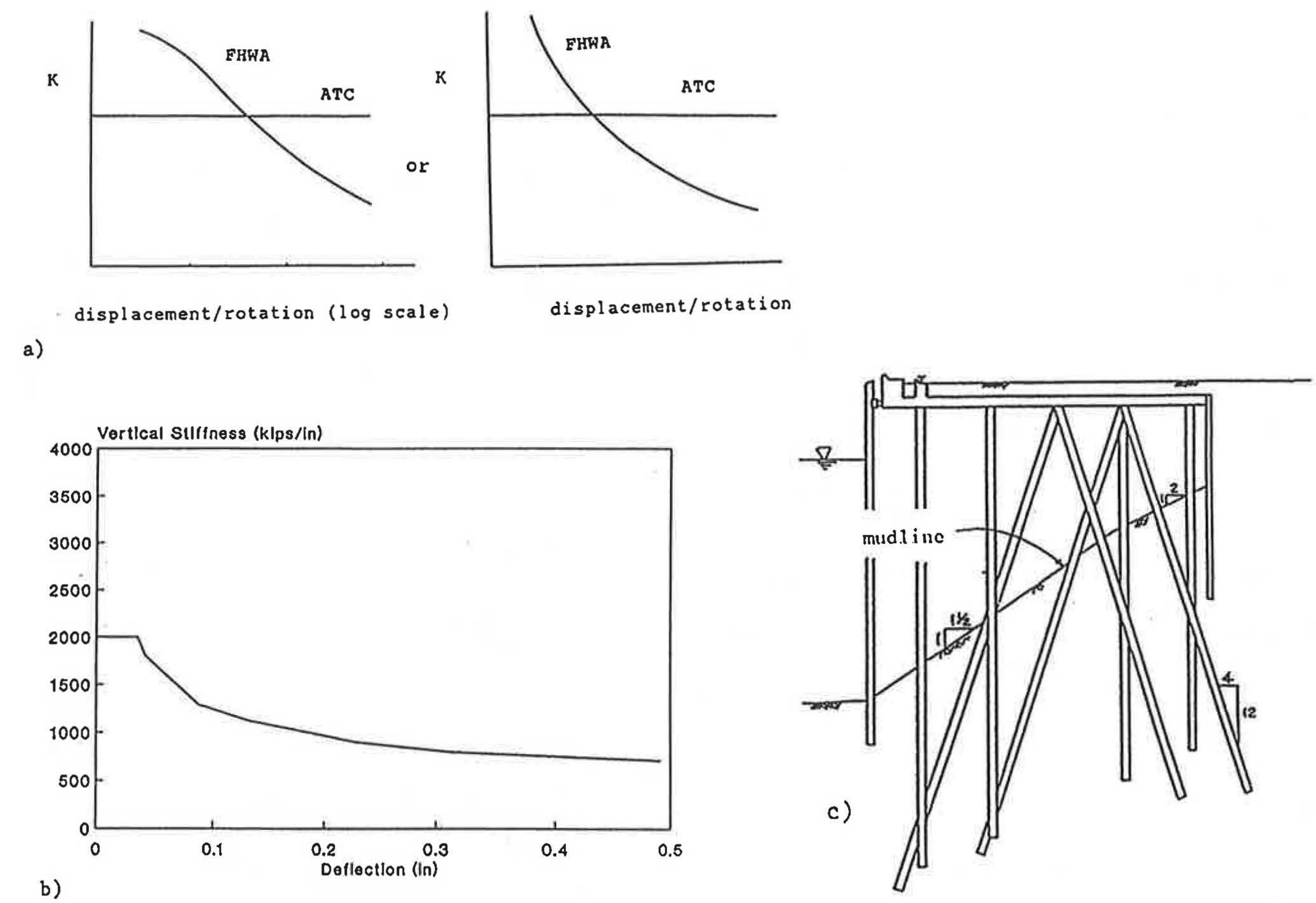

FIGURE 10 (a) Stiffness variation by FHWA versus ATC approaches; (b) proposed pile stiffness variation, as shown here for axial stiffness of all 18-in.-square prestressed concrete piles at (c) Oakland Outer Harbor for the Loma Prieta earthquake.

ure 10c is a cross section of the wharf, which is basically a long, free-standing pile group with batter piles. However, because of the flexibility of the wharf deck and the presence of batter piles, recorded transverse free-field motions were applied to a three-dimensional finite element model of the unsupported length of the piles and deck through lateral and vertical springs (a pair for each pile) at the mudline. Curves of the type shown in Figure 10b were developed (one vertical/axial stiffness curve for all piles and different lateral stiffness curves, not shown, depending on the force/moment condition at the mudline applicable to each pile). Several finite element runs were required before displacement compatible spring stiffnesses were assumed. Once this was accomplished, a comparison of the predicted and the recorded transverse accelerations at recording stations on the deck yielded a nearly perfect match. However, in obtaining compatible stiffnesses, it was noticed that the resulting vertical stiffness values all fell along the level portion of the vertical stiffness curve (Figure 10b) while the lateral stiffness values all fell on the descending portion of their respective curve. By contrast, use of stiffness values significantly different from such compatible values resulted in poor to very poor correlation between the recorded and the predicted accelerations on the deck.

SOIL-PILE FOUNDATION INTERACTION FAILURE

As mentioned earlier, if a soil from which a pile foundation derives some or all of its support softens significantly (or fails in part), a soil-foundation interaction failure may ensue. Such a softening response can occur in a loose to medium sand with developing porewater pressure that may not be sufficient to cause liquefaction but may be high enough to cause trouble. Likewise, under high static loads (e.g, friction piles in Mexico City), cyclic degradation of clay under seismic loading can lead to large displacements.

While it is possible to accommodate porewater pressure buildup in a lateral stiffness analysis by reducing the subgrade modulus profile of Figure 3a at each depth on the basis of the ratio of the reduced vertical effective stress to the original effective stress, once a zone liquefies, particular attention should be paid to whether the piles can take the bending/shear deformation across that layer. The load on such a pile would then include the inertia effects of the soil above the liquefied zone.

Nonstable rotational stiffness, on the other hand, develops when the piles of one or more rows reach axial pile capacity in either tension or compression. Once moment, M, causes such a response, the piles of that row plunge or pull out, that is, they experience a large plastic displacement, Δz, at a constant axial resistance, $Q = Q_{ult}$, until moment, M, reverses. The Q-z travel paths of such piles never stabilize, and both the Q-z response of the piles and the M-θ behavior of the group become a function of the pattern (as well as the magnitude) of the inertial interaction loading (i.e., the θ or M versus time, t, response as well as the θ or M amplitude). Consequently, the rotational stiffness, K_θ, of the pile group cannot be assessed a priori, that is, without knowledge of the free-field motion, because the pattern of inertial interaction loading, M versus t, or excitation, θ versus t, is dependent on the response of the superstructure to the free-field response.

Norris (*2*) provides an analysis of such nonstable rotational behavior of the central pier pile group of the Meloland Overcrossing during the 1979 Imperial Valley earthquake, including a comparison of the evaluated stiffness with the back-calculated value from system ID analysis of the recorded response of the bridge (*8*). By contrast, the rotational stiffness of the same foundation as tested under nonseismic conditions (*9*) is some 20 times higher. Norris et al. (*4*) provide a similar analysis of the lateral and rotational stiffnesses of the pile foundations of the Cypress Viaduct during the Loma Prieta earthquake.

SUMMARY

The information presented is an overview of recent studies (*1–4*) of a methodology for lateral and rotational stiffness evaluation and field case study comparisons. The methodology is an alternative to stiffness evaluation approaches adopted by FHWA and ATC. Of course, it is the author's strong belief that such evaluation should be undertaken or overseen by a geotechnical engineer given his appreciation for the level of free-field soil strains, soil's nonlinear stress-strain behavior, and the possibility of developing pore pressures in sand or cyclic degradation of clay under seismic excitation, or both.

The recommended lateral stiffness evaluation procedure is an equivalent linear subgrade modulus profile approach that is intended to be more accurate than existing p-y curve analysis at seismic levels of excitation. The proposed procedure accounts for the embedment of the pile heads, the group interference effect, and the pile cap contribution in contrast to other approaches, which only allude to these effects (or, in the case of the pile cap, wrongly assess a base shear resistance). This nonlinear stiffness evaluation procedure requires only hand computations (assuming prior knowledge of free-field strains) and takes only slightly longer than the time necessary to establish the so-called design level stiffness.

The basic rotational stiffness evaluation procedure assumes nonlinear stabilized response, from which it is a simple matter to evaluate the corresponding level of (permanent) rotationally induced settlement that occurs. The dead load on the structure influences whether nonstable behavior occurs as the result of compressional or tensile pile capacity failure. If nonstable rotational behavior develops, the Q-z travel paths that result are a direct function of the pattern as well as the amplitude of inertial interaction loading as demonstrated elsewhere for the case of the Meloland Overcrossing. Whereas some may wish to avoid nonstable behavior altogether, a more practical approach might be to design to accommodate a certain amount of deformation (as with abutment wall movement).

REFERENCES

1. G. M. Norris. Foundation Stiffness Evaluation for Seismic Analysis of Highway Bridges. *Proc., 23rd Symposium on Engineering Geology and Soils Engineering*, Logan, Utah, April 1987, pp. 375–394.
2. G. M. Norris. A Seismic Analysis: Meloland Overcrossing During the 1979 Earthquake. *Soil Properties Evaluation from Centrifugal Models and Field Performance*. Geotechnical Special Publication 17, ASCE, 1988, pp. 88–117.
3. G. Norris et al. *Soil-Foundation-Structure Behavior at the Oakland Outer Harbor Wharf*. Report 91-2. Center for Civil Engineering Earthquake Research, University of Nevada, Reno, June 1991.
4. G. Norris et al. *Seismic, Lateral and Rotational Pile Foundation Stiffnesses at Cypress*. Report 91-3. Center for Civil Engineering Earthquake Research, University of Nevada, Reno, July 1991.
5. I. Lam and G. R. Martin. *Seismic Design of Highway Bridge Foundations*. Reports FHWA/RD-86/101, FHWA/RD-86/102, and FHWA/RD-86/103. FHWA, U.S. Department of Transportation, June 1986.
6. B. M. Douglas and J. A. Richardson. Maximum Amplitude Dynamic Tests of a Highway Bridge. *Proc., 8th World Conference on Earthquake Engineering*, Vol. 6, 1984, pp. 889–896.
7. *Tentative Provisions for the Development of Seismic Regulations for Buildings*. ATC 3-06. Applied Technology Council, 1978.
8. B. M. Douglas, G. M. Norris, L. Dodd, and J. Richardson. Behavior of the Meloland Road Overcrossing During the 1979 Imperial Valley Earthquake. *Proc., 16th Joint Meeting of the U.S./Japan Panel on Wind and Seismic Effects*, UJNR, May 1984, 27 pp.
9. E. A. Maragakis, B. M. Douglas, and S. Vrontinos. Experimental and Analytical Soil-Structure Interaction Studies of Meloland Road Overcrossing. Accepted for 1992 ASCE Structures Congress.

Publication of this paper sponsored by Committee on Foundations of Bridges and Other Structures.